Improving the DDA Solution Time by Modifying the Contact Enforcement Technique

M.S. Khan[2], A. Riahi[1,] & J.H. Curran[1, 3]
1. Rocscience Inc., Toronto
2. Schlumberger Canada Ltd.
3. Professor Emeritus, Civil Engineering Department & Lassonde Institute, University of Toronto

ABSTRACT

This paper will focus on the efficiency of Discontinuous Deformation Analysis (DDA) applied to jointed rock problems. DDA uses an implicit time-integration scheme to solve the governing equations of motion through time. It therefore requires forming global system of equations. In recent studies, the authors have shown that although theoretically there is no restriction on DDA time-step size, DDA-Shi is in fact slower than methods that utilize an explicit time integration scheme. The observed slowness in the DDA solution of real-scale geotechnical problems is caused by the combination of the highly nonlinear nature of contact problems and the size of the global system of equations in implicit time integration techniques. This paper will focus on improving the computational efficiency of DDA-Shi by adopting a concept similar to the soft contact approach. It will be shown that by removing the no-penetration constraint of the contact penalty enforcement in DDA-Shi, the solution time decreases significantly. The conclusions are verified in examples that examine the stability of slopes in jointed rock masses.

RÉSUMÉ

Cet article mettra l'accent sur l'efficacité de l'analyse de la déformation discontinue (ADD) appliqués aux problèmes des roches démontables. L'ADD utilise un système d'intégration temporelle implicite pour résoudre les équations qui gouvernent le mouvement à travers le temps. Il faut donc former un système global des équations. Dans des études récentes, il a été démontré que même si théoriquement il n'y a aucune restriction sur la taille du temps-étape de l'ADD, l'AAD-Shi est effectivement plus lente que les méthodes qui utilisent un système d'intégration temporelle explicite. La lenteur observée dans la solution des problèmes géotechniques d'échelle réelle dans l'ADD est causée par la combinaison de la nature des problèmes de contact, qui sont extrêmement non-linéaire, et de la taille du système global des équations dans les techniques d'intégration temporelle implicite. Cet article se concentrera sur l'amélioration de l'efficacité de calcul de l'ADD-Shi en prennant un concept similaire à l'approche du contact souple. Il sera démontré que, en supprimant la contrainte de non-pénétration de l'application des peines du contact, le temps de la solution diminue de manière considérable. Les conclusions sont vérifiées dans les exemples qui examinent la stabilité des pentes dans les masses de roches démontables.

1 INTRODUCTION

In recent years, much attention has been focused on efficient numerical techniques for analyzing jointed rock problems. The presence of joints in rock masses results in discontinuous behavior, and gives rise to failure mechanisms that vary with scale. There are two approaches to the numerical analysis of jointed rock problems: continuum-based methods and discrete techniques.

This paper will focus on the latter category of computational methods. In discrete element techniques, jointed rock masses are modelled as assemblies of discrete blocks that may be rigid or deformable. In geotechnical problems, the Discontinuous Deformation Analysis (DDA) and the Distinct Element Method (DEM) are often identified as the two most widely-used discrete element techniques (Jing, 2007).

DDA uses an implicit time-integration scheme to solve the governing equations of motion, namely conservation of linear and angular momentum, through time. It therefore requires forming a global system of equations. DEM, on the other hand, applies explicit time integration and thus can solve the equations of motion locally.

The computational efficiency of DDA and DEM is the main determinant in choosing between them as a solution tool for engineering scale geotechnical problems. Computational efficiency is defined as the computational speed in terms of CPU time required for the analysis. It has been argued in literature that DDA is unconditionally stable due to its use of implicit time integration, and is faster than conditionally stable time integration techniques because it can accommodate considerably larger time steps. Theoretically, it is therefore expected that DDA will solve jointed rock problems more efficiently than DEM.

In a recent work, we investigated the expected benefits of DDA (Khan, 2010; Khan et al., 2010). We performed a systematic study on the factors that affect the solution time, including the time step size, type of matrix solver, contact search algorithm, and contact resolution technique. The comparison was performed using two representative software tools, namely the original DDA developed by Shi (DDA-Shi), and UDEC, developed by Itasca (2004). It was concluded that although theoretically there is no restriction on DDA time-step size, DDA-Shi is actually slower than methods that utilize an explicit time integration scheme.

The observed slowness in the DDA solution of real-scale geotechnical problems is caused by the combination of the highly nonlinear nature of contact problems and the size of the global system of equations in implicit time integration techniques. In DDA-Shi, the no-penetration constraint is satisfied in an iterative manner referred to as the open-close iterations. Due to its use of implicit time integration, the global system of equations needs to be rebuilt at each iteration of the DDA solution, which demands considerable time.

This paper will focus on improving the computational efficiency of DDA-Shi by adopting a concept similar to the soft contact approach used in UDEC. It will be shown that by removing the no-penetration constraint of the contact penalty enforcement, the solution time decreases significantly. These conclusions will be verified in examples that examine the stability of slopes in jointed rock masses.

2   INTRODUCTION TO DEM AND DDA

The equations governing the behavior of a system of discrete blocks are the conservation of mass, conservation of linear and angular momentum, and the material constitutive equations. The motion and deformation of each individual block in a discrete system follows from the conservation of linear and angular momentum equations. The conservation of linear momentum equation is expressed by

$$-\frac{\partial u_j^2}{\partial t^2}\rho + \sigma_{ij,i} + b_j = 0 , \tag{1}$$

where $\mathbf{u}$ is the displacement, $\boldsymbol{\sigma}$, the Cauchy stress tensor, $\mathbf{b}$, the body force, and ρ, the density of material.

The original DEM assumes that the blocks are rigid. The displacement field over each rigid block can then be represented by the rigid body displacement of a reference point on the block and the rotation of the discrete body about this point. To determine block rotations, the equation of angular momentum needs to be explicitly solved. DDA-Shi uses a first-order interpolation function to approximate the deformation field of a block from block vertex displacements. The displacement field over a block is then represented by displacement of a reference point on the block, rotation of the block about the axes passing through the reference point and a constant strain field.

However, similar to rigid block DEM, since the motion of a volume is expressed by motion of a point, equilibrium of angular momentum needs to be explicitly satisfied to determine the rotation of the block. In this work we have assumed that the DDA blocks are rigid. Details on how to implement this assumption are discussed in [Koo, 1998; Khan, 2010]. By enforcing this assumption the number of degrees of freedom for a given block assembly will become identical in rigid block DDA and DEM. This eliminates the contributions that differences in the size of the system of equations can have on the solution time.

DEM uses an explicit central difference time-marching scheme to solve the governing equations of motion through time. In the central difference scheme, the equilibrium of the system at time t is considered to calculate the displacement at time $t+\Delta t$. The solution for the nodal point displacements at time $t+\Delta t$ is obtained using the central difference approximation for the accelerations, $\ddot{\mathbf{u}}_i^t$.

In general, the mass matrix on the left-hand side can be represented as a diagonal matrix. Equation (1) therefore can be rearranged as

$$m_i\ddot{\mathbf{u}}_i^t = (\mathbf{F}_i^t)^{out-of-balance} , \tag{2}$$

where i represents the index of the degree of freedom. For the particular case of rigid block DEM, m_i becomes the mass of each block. The uncoupling of the equations of motion, which is one of the major advantages of explicit integration schemes, eliminates the need for assembly of global mass or stiffness matrices and inversion of the global matrices.

In rigid block DEM, at each time step, the kinematic variables, i.e., accelerations, velocities and displacements, are first calculated using a central difference scheme, and the dynamic quantities (contact forces or stresses, as well as internal stresses of the elements) are then obtained by invoking the constitutive relations for the contacts and the block materials.

$$\dot{u}_{(t+\Delta t/2)}^i = \dot{u}_{(t-\Delta t/2)}^i + \left(\sum F_t^i / m + g^i\right)\Delta t \text{ , and} \tag{3}$$

$$\dot{\theta}_{(t+\Delta t/2)}^i = \dot{\theta}_{(t-\Delta t/2)}^i + (\sum M_t / I)\Delta t ,$$

where $\sum F_t^i$ is the sum of all the forces acting on the block including the damping force, $\dot{\theta}$ is the angular velocity of the block about its centroid, ΣM is the total moment acting on the block, $\dot{u}^i$ is the velocity components of the block centroid, and g_i is the components of gravitational acceleration (body forces). Explicit time integration is conditionally stable, which requires that the time-step size must be smaller than a certain critical value, Δt_c, for numerical errors not to grow unbounded. The critical time step is related to the time it takes for stress waves to travel across a block.

$$\Delta t_c \leq 2/\omega_{max} , \qquad (4)$$

where ω_{max} is the highest eigenfrequency of the system.

DDA uses an implicit time marching scheme. Different variations of implicit time integration schemes have been developed. In implicit time integration schemes, acceleration and velocity components are expressed in terms of displacement components. In general terms, the displacement at time $t + \Delta t$ is obtained by

$$\hat{\mathbf{K}}\Delta\mathbf{u}^{t+\Delta t} = \Delta\mathbf{F}^{t+\Delta t} \text{, or} \qquad (5)$$
$$\left[\frac{2\mathbf{M}}{\Delta\mathbf{t}^2} + \frac{2\mathbf{C}}{\Delta\mathbf{t}} + \mathbf{K}\right]\mathbf{u_{n+1}} = \mathbf{F_{n+1}} + \frac{2\mathbf{M}}{\Delta\mathbf{t}}\dot{\mathbf{u}}_\mathbf{n} + \mathbf{C}\dot{\mathbf{u}}_\mathbf{n} ,$$

The solution of Equation (5) requires assembling the global mass and stiffness matrices and solving the coupled system of equations using a direct matrix inverse operation or an iterative solver. The global stiffness matrix, $\mathbf{K}$, includes the sub-matrix representing deformability of blocks and contacts, with contact matrices as off-diagonal terms.

DDA uses the Newmark-β method (Wang et al., 1996), one of the generalized Newmark integration schemes, which provides algorithmic damping (numerical dissipation). Therefore, the explicit damping term, C, in DDA-Shi is assumed to be zero.

2.1   Contact Treatment in DDA-Shi and DEM

Mathematically, contact is treated as a constraint on displacements at the interface between two objects. A normal contact constraint prevents interpenetration of objects, while a tangential constraint enforces sticking/slipping.

DDA-Shi uses penalty enforcement of contact constraints (Mohammadi, 2003; Wriggers, 2002). The penalty method satisfies these constraints approximately. The approximate enforcement of a constraint is achieved through a proportionality law or penalty function that relates the degree of constraint violation to the size of the corrective measure. Any surface penetration violates the impenetrability constraint and invokes contact forces that tend to return the surfaces to a state of compliance with the imposed constraints. Similarly, tangential penalty forces are developed as a result of relative tangential displacements at the contacting surfaces. From the approximate enforcement of the normal impenetrability and tangential sticking constraints, the following potential energy terms arise:

$$\Pi^{contact} = \frac{1}{2}d_n^2\alpha_n + \frac{1}{2}d_t^2\alpha_t , \qquad (6)$$

where d_n and d_t are the normal and tangential displacements of a contact point on the boundary, measured with respect to the target surface with normal $\mathbf{n}$, α_n and α_t are the normal and tangential penalty coefficients, respectively, in force/length dimensions.

DEM, uses the soft (compliant) contact approach (Itasca, 2004). In this approach, penetration displacements are not constrained. This approach assumes that springs exist at the contacts, and permits infinitesimal penetrations. Associated forces are then calculated using the constitutive laws of the springs. Assuming a linear constitutive spring relationship, $F = k\Delta l$, the potential function for each contact point becomes

$$\Pi^{contact} = \frac{1}{2}(k_n d_n^2 + k_t d_t^2) , \qquad (7)$$

were k_n and k_s are the normal and shear stiffness at the contact, respectively.

Since DDA enforces the no-penetration constraint approximately, it requires a number of iterations to adjust the penetration distance to a specified value. In addition, because of its implicit integration technique, DDA requires that both the force vector and stiffness matrix be calculated. Minimization of potential energy with respect to displacements gives the stiffness and force terms arising from contact (Shi, 1988; Khan, 2010, Riahi et al. 2010).

UDEC is based on a soft contact approach, and does not enforce the no-penetration constraint. Also, since the method uses an explicit time integration, calculation of contact stiffness is not required, and forces can be directly calculated by evaluating the penetration and relative tangential distances using $F_n = k_n d_n$ and $F_s = k_t d_t$.

It has been discussed by Khan(2010) that both DDA-Shi and UDEC apply a similar technique for contact resolution by classifying contact modes as node-to-node, node-to-edge, and edge-to-edge and evaluating the penetration distance. Therefore, it can be concluded that the differences between the contact formulations of the two methods arise from (i) calculation of the contact stiffness matrix in DDA-Shi, which is an inherent requirement for implicit time integration, and (ii) enforcement of a threshold for normal penetration in DDA, which results in an iterative procedure often referred to as "open-close" iterations.

2.2   Modification of DDA with Soft Contact Approach

As discussed in Section 2.1, the hard contact approach used in DDA prevents the overlap or interpenetration of the blocks by using penalty springs. Contact convergence is therefore achieved iteratively. There are two major disadvantages to this approach; one is related to the penalty value and the second to satisfying the no-penetration constraint.

The penalty value can significantly affect the computational efficiency of DDA (refer to Khan, 2010,

Chapter 3). An inappropriate penalty value may destroy the conditioning of the global stiffness matrix, thus affecting the convergence of the solution. In addition, it is difficult to estimate an appropriate penalty value for an arbitrary problem. Alternative approaches such as the classical Lagrange multiplier method and the augmented Lagrange method also havesome disadvantages. The classical Lagrange multiplier method adds a gap parameter for each contact, creating a larger system of equations and the augmented Lagrange method requires more iterations to reach convergence, increasing the solution time and consequently, the computational cost.

In DDA-Shi, the no-penetration contact constraint is imposed at each contact point. To satisfy this constraint, the iterative solver proceeds until there is no penetration at any contact point. Achieving zero-penetration is impractical. In order to avoid this problem, Shi defined a penetration control parameter or penetration tolerance (f_0). Contact convergence and the final solution largely depend on the value of f_0. Very small tolerance values can lead to fluctuation of results or even divergence of the solution, and large tolerance values may produce incorrect contact forces. In addition, it is difficult to determine an acceptable tolerance value for an arbitrary problem.

In addition, satisfying the no-penetration constraint at every contact point is a time-consuming process because of the need to form and solve a large system of equations using an iterative process. The no-penetration approach may exhibit fluctuating divergence for problems involving large numbers of blocks or contact points (Khan, 2010, Chapter 3). It has been shown that the number of open-close iterations required for contact convergence in each time step dramatically increases for problems involving more than 500 blocks. As the number of open-close iterations increases the computational cost also increases.

These aforementioned disadvantages make DDA's hard contact approach computationally expensive. Moreover, the assumption that contacts are infinitely rigid is unrealistic because blocks undergo some local deformation at contact points that must be accounted for. In this work, we adopted the concept of soft contact by allowing interpenetration or overlapping of the contacting blocks (DDA-SC). To do so, a normal contact spring with finite stiffness is used to represent the measurable stiffness at a contact point (see Fig. 1) Details of implementation are discussed in (Khan, 2010).

Although physically, overlapping and interpenetrations of blocks do not occur, small numerical interpenetration can be interpreted as the actual surface deformation at contact points. The joint stiffness properties can be obtained from laboratory and field testing.
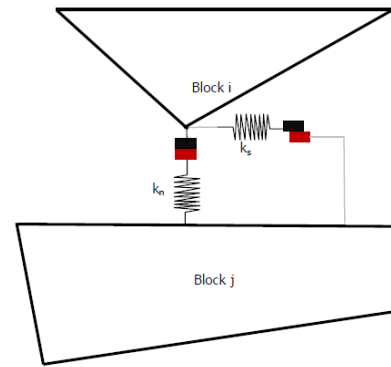
Figure 1. Contact representation in DDA-SC

3   EXAMPLES

In this Section, the improvements in the computational efficiency of DDA-SC over DDA-Shi are demonstrated through four examples. The examples involve simple case of block sliding as well as large scale slope stability problems.

3.1   Block on an Inclined Surface

The benchmark example involves a rigid block sliding on an inclined plane (Fig. 2). The unit depth rectangular block has a length 2.0 *m* and height 1.0 *m*, and lies on an inclined surface with a slope angle, α. The friction angle between the block and the inclined surface is specified through the joint friction angle, ϕ. The aspect ratio of the block and orientation were chosen such that the mode of failure is sliding. Due to gravitational forces, the block on the inclined plane will accelerate down the plane. In DDA-SC model, normal and shear contact spring stiffness, k_n and k_s, equal to 50 *MPa/m* are used.

The analytical solution for the displacement, *d*, of the block centroid relative to its at-rest position is given by

$$displacement\ (d) = \begin{cases} 0 & \phi > \alpha \\ \frac{1}{2}g(\sin\alpha - \cos\alpha\ \tan\phi)t^2 & \phi < \alpha \end{cases} \tag{8}$$

Using DDA-SC, for five different cases that involve a range if friction angles and a slope angle of 30°, the block centroid displacement is computed. The solution is compared to that obtained from DDA-Shi.

The block centroid displacement as a function of time is shown in Fig. 3. It is observed that DDA-SC captures an essential aspect of problem behavior in the sliding process: namely, the displacement reduces as the friction angle increases. Fig. 4 shows the residual error, $e = \left| d^{Anal} - d^{DDA} \right|$, with respect to time. It can be interpreted form this figure that DDA's solution error grows linearly in time. Although for both the soft and the hard contact approaches the error is linear with respect to time, the hard contact approach solution deviates more from the analytical solution. DDA-Shi has an error less than 2% for

this problem whereas the DDA-SC exhibits an error less than 1%. It can therefore be concluded that the soft contact approach has improved the accuracy of DDA.
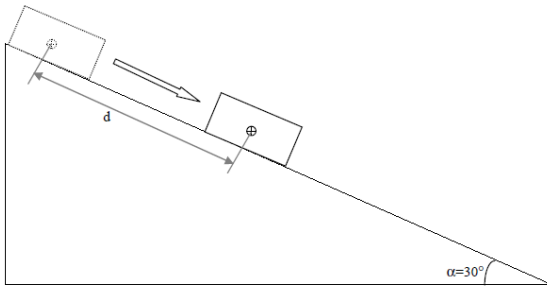
Figure 2. Block sliding on inclined surface (problem geometry)
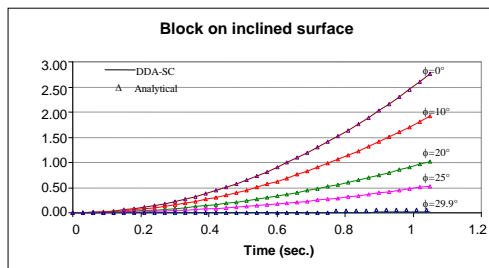
Figure 3. Block sliding on inclined surface (displacement vs. time)
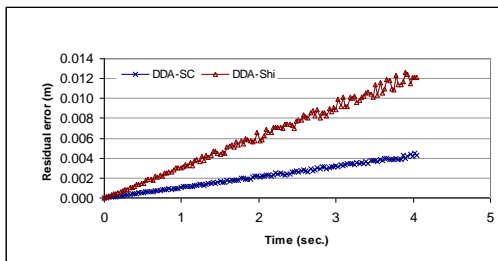
Figure 4. Residual error in displacement using DDA-SC and DDA-Shi

3.2 Plane Failure Slope Stability

This example intends to show the accuracy and reliability of the enhanced DDA solution in a simple slope stability example exhibiting planar failure. The problem geometry is depicted in Fig. 5. The slope has a height of 60 meters, a slope face angle, α, of 50°, and joint failure plane dipping at 35°. The block and joint material properties are listed in Table 1. The joint exhibits Mohr-Coulomb elasto-plastic behavior. The analytical solution for the stable state can be obtained by comparing the driving forces and the resisting forces developed along the joint.

In order to compute the Factor of Safety (FOS), the Shear Strength Reduction (SSR) procedure (Diederichs et al., 2007; Hammah et. al., 2004) is implemented in DDA-SC. SSR is a simple approach that involves a systematic search for a strength reduction factor (SRF) that brings a slope to failure. For the detailed procedure

of the implementation of the SSR technique in DDA, refer to (Khan, 2010).

Fig. 6 demonstrates the displacement vs. Shear Reduction Factor (SRF) for a selected point on the block. The displacements are obtained at 1000 time step. The results indicate the SRF that brings DDA-SC solution of this example to instability is 1.829. The prediction is in good agreement with the analytical solution of 1.835.
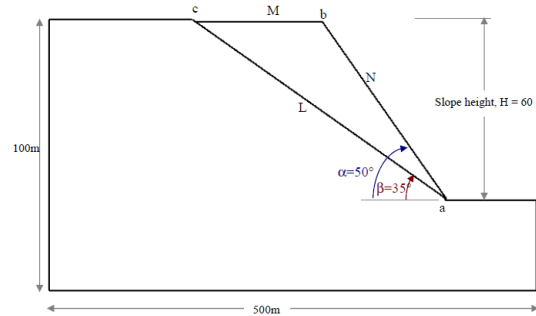
Figure 5. Plane failure slope stability geometry
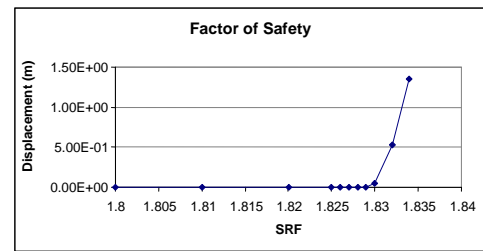
Figure 6. Displacement of measured point vs. SRF using DDA-SC

Table 1. Input parameters used in DDA-SC

Material properties
Unit weight, $\gamma = 0.027$ _MN/m³_
Joint friction angle, $\phi = 40°$
Joint cohesion, c = 0.1 _MN/m²_
Tensile strength, $\sigma_t = 0$
DDA-SC parameters
$k_n = 1$ GPa/m and $k_s = 0.1$ _GPa/m_
Time step, $\Delta t = 0.001$
$\Delta_{umax} = 1E-05$ _m_
Gravity, g = 10 _m/sec²_

3.3 Plane Failure Slope Stability Involving Multiple Blocks

This problem involves a slope with a parallel set of joints spaced 10 _m_ apart dipping out of the slope at 35.2°(Fig. 7) The slope has a height of 260 _m_ and a slope face angle, α, of 55°. Parallel joints split the rock mass into 28 discrete blocks, which are considered to be rigid. The material properties are listed in Table 2.

This example intends to show how well DDA-SC can handle problems with multiple blocks. For comparison purposes, a UDEC analysis was performed. The input

parameters used in DDA-SC and UDEC are listed in Table 2.

The closed-form solution for this problem (Khan, 2010) gives a factor of safety of 1.3092. The UDEC analysis predicts a factor of safety, 1.3, and a planar failure mechanism that involves sliding along a joint near the slope toe (see Fig. 7). The DDA-SC analysis predicts the factor of safety to be 1.296. Comparison of results confirms that that DDA-SC can predict the mechanism of deformation and failure correctly and within the desirable level of accuracy.
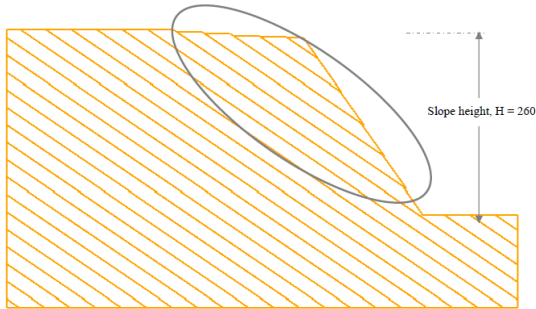
Figure 7. Planar failure slope example (multiple blocks)

Table 2. Input data used for verification Example 3.3

Material properties	
Unit weight, γ = 0.0261 MN/m^3 Joint friction angle, ϕ = 40° Joint cohesion, c = 0.1 MN/m^2 Tensile strength, σt = 0 Gravity, g = 10 m/sec^2	
DEM input parameters	**DDA-SC input parameters**
k_n = 1 GPa/m k_s = 1 GPa/m Time step, Δt = 0.000873	k_n = 1 GPa/m k_s = 1 GPa/m Time step, Δt = 0.001 Δu_{max} = 1E-05 m

3.4 Slope Stability Involving Two Joint Sets

A slope with a height of 260 m and a slope face angle of 55° is considered. It has two sets of intersecting joints, a set of horizontal joints with 40 m spacing and a set parallel to the slope face with 10 m spacing as shown in Fig. 8. This slope stability problem was analyzed by DDA-SC and UDEC. Block material properties and input parameters used in the DDA-SC and UDEC analyses are given in Table 3.

The constitutive behavior of the joints follows a Mohr-Coulomb failure criterion. The SSR procedure is used to estimate the factor of safety. Using UDEC, initially, the steady state or equilibrium state of the problem is achieved, and subsequently, the Mohr-Coulomb strength parameters are repeatedly reduced until the analysis fails to reach equilibrium state. The equilibrium condition is considered to be achieved when the unbalanced force is less than a specified tolerance

within a specified number of time steps. For this problem, the limiting unbalanced force was set to be 1.0 kN and the limiting number of time steps was set to be 10000.
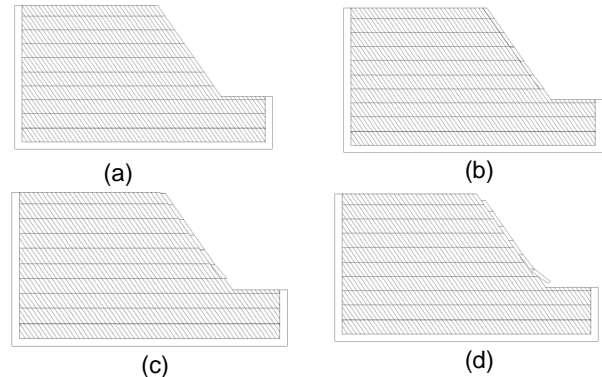
Figure 8. Slope stability simulation in DA-SC (a) Step = 1 (initial geometry), (b) Step = 1522 (failure initiates), (c) Step = 3300 (block sliding) (d) Step = 9100 (block sliding and rotation)

Table 3. Input data used for verification Example 3.4

Material properties	
Unit weight, γ = 0.0261 MN/m^3 Joint friction angle, ϕ = 40° Joint cohesion, c = 0.1 MN/m^2 Tensile strength, σ_t = 0 Gravity, g = 10 m/sec^2	
UDEC input parameters	**DDA-SC input parameters**
k_n = 10 GPa/m k_s = 10 GPa/m Time step, Δt = 0.0069 Damping = auto damping option used	k_n = 10 GPa/m k_s = 10 GPa/m Time step, Δt = 0.001 Δu_{max} = 1E-05 m

In DDA-SC, the input parameter for relative maximum displacement is used to judge the limit equilibrium state (Shi, 2007). When the relative maximum displacement is less than the specified tolerance, the system is assumed to have attained steady state. As mentioned before, to compute the factor of safety using SSR method, a separate function is incorporated into the existing DDA code. Similar to the UDEC methodology, the DDA analysis is first run until steady state is attained and then the shear strength parameters are systematically reduced until it does not attain steady state within a prescribed maximum number of time steps. The maximum number of time steps is set to be twice the number of time steps required to attain steady state in the beginning of the analysis.

Fig. 8 illustrates the DDA-SC analysis of this problem at various critical states during the analysis. The time-step size used for the analysis was 0.001 second. At time step=1522 failure is initiated by sliding of a block at the toe of the slope. DDA-SC predicts a failure mechanism which is initiated by sliding and then by rotation of the block nearest to the slope toe. DDA-SC

predicted a factor of safety of 1.82. The failure mechanism predicted by DDA-SC is shown in Fig. 9(a). The UDEC analysis predicted a similar failure mechanism, and a factor of safety of 1.74 shown in Fig. 9(b). The difference between the factors of safety predicted by DDA-SC and UDEC is approximately 3.5%.

(a)	(b)
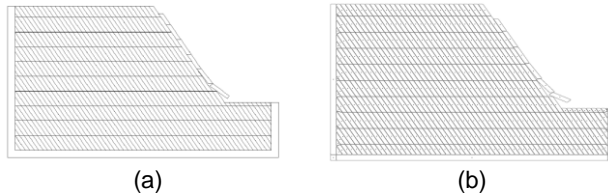
Figure 9. Comparison of slope failure mechanism in DDA-SC and DEM (a) Slope failure predicted by DDA-SC (b) Slope failure predicted by UDEC

For comparison purposes, this slope problem was also analyzed by DDA-Shi, which predicts a similar failure mechanism and a factor of safety of 1.80. The final results obtained by UDEC, DDA-Shi and DDA-SC are provided in Table 4. Comparison of results confirms that hard contact and soft contact logics used in enforcement of contact constraints lead to convergence to one physically admissible solution. In terms of computational speed, DDA-Shi took approximately 25 minutes of CPU time to attain limit equilibrium state whereas DDA-SC took approximately 6 minutes (refer to Table 4). Results indicate that soft contact implementation improved the computational efficiency of DDA. DDA-SC, however, could not match the speed of DEM which reached equilibrium in less than one minute.

Table 4. Comparison of results from DDA and UDEC for Example 3.4

Aspect		DDA-Shi	DDA-SC	UDEC
Problem size	Blocks	482	482	468
	DOFs	1446	1446	1404
Analysis result	Failure mechanism	Block sliding and rotation	Block sliding and rotation	Block sliding and rotation
	Factor of safety	1.80	1.82	1.74
CPU time (min.)	Steady state	25	6	1
	Post failure			
	10 m	47.3	10.4	2.8
	20 m	65.4	17.8	4.3
	30 m	78.7	25.3	5.7
	40 m	98.2	29.6	7.2
	Average 25 m	72.4	20.8	5.0

It has been discussed that application of discrete element techniques is most desired when large deformation, including sliding or rotation of blocks are a dominant mechanism in the response. Therefore, the capability and efficiency of discrete element methods in the post-failure regime is an integral part of the evaluation of discrete methods. The efficiency of the DDA solution in the post-failure regime is investigated by recording the CPU time for four different "physical times" (see Table 4). The times associate with a block displacement of 10 *m*, 20 *m*, 30 *m*, and 40 *m*.

The displacement versus CPU time for DDA-SC, UDEC, and DDA-Shi solutions are plotted in Fig. 10. This figure shows that compared to DDA-Shi, DDA-SC has improved the computational speed by a factor of four in modelling the post-failure behaviour. However, UDEC, which is based on the distinct element method, took an average of 5 minutes, i.e., four times faster than DDA-SC and 15 times faster than DDA-Shi.
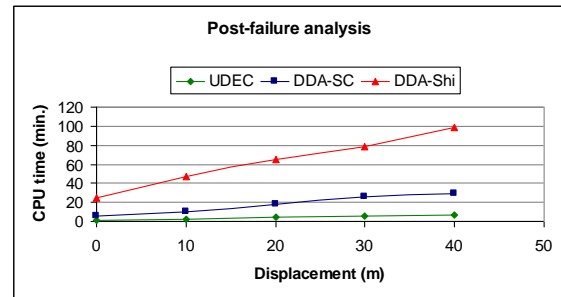
Figure 10. Comparison of time taken for post-failure analysis in Example 3.4

It has been shown by Khan et al. (2010) that for rigid blocks, DEM and DDA differ in their time integration scheme and their contact enforcement method. It can be argued that after incorporating the soft contact approach in DDA, the main difference between DEM and DDA-SC is the time integration scheme used, implicit versus explicit. Implicit time integration schemes require assembly of a global matrix to solve a coupled system of equations. Explicit time integration schemes lead to an uncoupled system of equations, which can be solved for each degree of freedom of a problem separately.

DDA requires that at each time step, a system of equations in the form of Equation (5) be solved iteratively. At each iteration of the solution, the global stiffness matrix is updated based on the updated position of block, and the position of the blocks is obtained by finding the solution to Equation (5). DDA-SC, therefore requires that the stiffness terms arising from contacting objects be incorporated in the global stiffness matrix. Any change in contact state results in nonlinear behaviour and changes in the global stiffness matrix. It is therefore expected that in systems where a large number of contacts are breaking and forming, multiple matrix inversions will be required during each time step.

During the post-failure state, new contacts are continuously forming and old contacts are breaking. This behaviour triggers continuous changes in the global stiffness matrix, and thus leads to slow convergence of the solution. Slow convergence increases the computational cost.

4 CONCLUSION

The hard contact approach used in DDA-Shi assumes contacts are rigid and does not allow penetration at the contact points. For this reason, overlap or interpenetration of the blocks is prevented using penalty springs and the contact convergence is achieved iteratively. There are two major disadvantages of this approach; one is related to the penalty value and the second to satisfying the no-penetration constraint.

This paper focused on improving the computational efficiency of DDA-Shi by adopting a concept similar to the soft contact approach used in UDEC. To implement a soft contact, the no-penetration constraint of the contact penalty enforcement was removed. In order to prevent large penetration of contacting objects, the time step size however was controlled. It was shown that such modification reduces the solution time significantly. The conclusions are verified in examples that examine the stability of slopes in jointed rock masses.

REFERENCES

Diederichs, M. S., Lato, M., Hammah, R. and Quinn, P. 2007. Shear Strength Reduction Approach for Slope Stability Analyses, Invited paper, 1st Canada-US Rock Mechanics Symposium, Vancouver, BC.

Hammah, R.E., Curran, J.H.,,Yacoub, T.E.,, and Corkum, B. 2004. Stability analysis of rock slopes using the Finite Element Method, Proceedings of the ISRM Regional Symposium EUROCK 2004 and the 53rd Geomechanics Colloquy, Salzburg, Austria.

Itasca Consulting Group. 2004. UDEC - Universal Distinct Element Code, Version 4.0 - User's Manual, Minneapolis, MN, USA.

Jing, L., Stephanson, O. 2007. Fundamentals of discrete element methods for rock engineering - Theory and Applications, *Developments in Geotechnical Engineering*, Elsevier, 85.

Khan, M.S. 2010. Investigation of discontinuous deformation analysis for application in jointed rock masses, Ph.D. Dissertation, University of Toronto.

Khan, M.S, Riahi, A., Curran, J.H., Effects of time step size on the efficiency of Discontinuous Deformation Analysis in jointed rock problems, *Proceedings of the 2010 ISRM Symposium and 6th Asian Rock Mechanics Symposium*, New Delhi, India, 2010.

Koo, C.Y., Chern, J.C. 1998. Modification of the DDA method for rigid block problems, *International Journal of Rock Mechanics and Mining Sciences*, 35(6):684–693.

Mohammadi, S. 2003. *Discontinuum mechanics: Using Finite and Discrete Elements*, WIT Press, Southhampton, UK.

Riahi, A., Curran, J.H., Hamma, R. 2010. Limits of applicability of the finite element explicit joint model in the analysis of jointed rock problems, *Proceedings of the 44th ARMA Conference*, Salt Lake City, UT, USA.

Shi, G.H. 1993. Block system modeling by discontinuous deformation analysis, *Computation Mechanics*, Southampton, UK.

Shi, G.H. 2007. Application of Discontinuous Deformation Analysis (DDA) to rock stability analysis, *Proceedings of 8th international conference on analysis of discontinuous deformation – Fundamentals & Application to mining and civil engineering* (*ICADD-8*), Beijing, China.

Shi, G.H. 1988. Discontinuous Deformation Analysis, Ph.D. thesis, University of California, Berkeley, USA.

Wang, C.Y., Chuang, C.C., Sheng, J. 1996. Time integration theories for the DDA method with finite element meshes, *Proceedings of 1st Int. Forum on Discontinuous Deformation Analysis (DDA) and Simulations of Discontinuous Media*, TSI, Berkeley, CA, USA. 263–287,

Wriggers, P. 2002. *Computational contact mechanics*, John Wiley & Sons, Hoboken, NJ, USA.